Critical state model with anisotropic critical current density

2003 J. Phys.: Condens. Matter 15 1325

(http://iopscience.iop.org/0953-8984/15/8/316)

INSTITUTE OF PHYSICS PUBLISHING JOURNAL OF PHYSICS: CONDENSED MATTER

J. Phys.: Condens. Matter **15** (2003) 1325–1337 PII: S0953-8984(03)57727-X

Critical state model with anisotropic critical current density

K V Bhagwat, Debjani Karmakar and G Ravikumar

Technical Physics and Prototype Engineering Division, Bhabha Atomic Research Centre, Trombay, Mumbai 400085, India

Received 30 December 2002
Published 17 February 2003
Online at stacks.iop.org/JPhysCM/15/1325

Abstract

Analytical solutions of Bean's critical state model with critical current density $\boldsymbol{J}_c$ being anisotropic are obtained for superconducting cylindrical samples of arbitrary cross section in a parallel geometry. We present a method for calculating the flux fronts and magnetization curves. Results are presented for cylinders with elliptical cross section with a specific form of the anisotropy. We find that over a certain range of the anisotropy parameter the flux fronts have shapes similar to those for an isotropic sample. However, in general, the presence of anisotropy significantly modifies the shape of the flux fronts. The field for full flux penetration also depends on the anisotropy parameter. The method is extended to the case of anisotropic $\boldsymbol{J}_c$ that also depends on the local field B, and magnetization hysteresis curves are presented for typical values of the anisotropy parameter for the case of $|\boldsymbol{J}_c|$ that decreases exponentially with $|B|$.

1. Introduction

Bean [1] proposed the critical state model (CSM) that provides a description of irreversible magnetization of hard type II superconductors. The model involves a material parameter, the critical current density $\boldsymbol{J}_c$. Solutions of CSM are available in the literature [2–7], for field independent as well as field dependent $\boldsymbol{J}_c$, for samples in parallel geometry where demagnetization factor $N = 0$ and also for perpendicular geometry where $N \neq 0$. In all these solutions the critical current density is assumed to be isotropic, i.e., $|\boldsymbol{J}_c|$ does not depend on the orientation of $\boldsymbol{J}_c$. Although the assumption of isotropy is valid for many real samples, there are situations where the assumption cannot be justified, especially for samples of high-T_c superconductors with field parallel to the ab-plane [8]. Sen *et al* [9] have recently measured the anisotropy in the critical current density in thin films of the newly discovered superconductor MgB_2 when the applied field is inclined to the c-axis. Schuster *et al* [10] have studied flux penetration into thin rectangular samples having anisotropic critical current density in the perpendicular geometry. This geometry pertains to $N \neq 0$. Here the effects of anisotropy are compounded with those due to a non-zero demagnetization factor. To study the effects of anisotropy alone, it would be instructive to analyse the problem for the $N = 0$ geometry.

0953-8984/03/081325+13$30.00

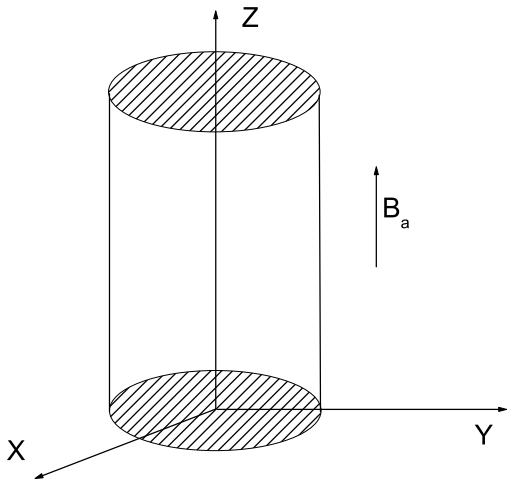

Figure 1. The parallel geometry for a cylindrical sample is shown. The cylinder is infinite in the z-direction. The long axis of the cylinder is parallel to the z-axis, which is also the direction of the applied field B_a.

In the present paper, we consider cylindrical samples of hard type II superconductors in a parallel geometry. The simple geometry brings out the essential features of anisotropy in $\boldsymbol{J}_c$ and, moreover, is amenable to an analytical treatment. The paper is organized as follows: in section 2, we present the formulation and a derivation of the general form of flux-fronts assuming arbitrary cross-section for the cylinder and also an arbitrary form of the anisotropy in $\boldsymbol{J}_c$. This should suffice for the calculation of magnetization curves. However, for the purpose of illustration, we have chosen elliptic cylindrical samples and the elliptic form [11] of anisotropy for $\boldsymbol{J}_c$. We present the details of our calculation for elliptic cylinders in section 3. In the next section we present our results and summarize our conclusions in the last section.

2. Formulation

Consider an infinite cylindrical sample of a hard type II superconductor subjected to a magnetic field B_a parallel to its axis that is taken to be the z-axis (figure 1). The magnetic field B within the sample is determined from the equations

$$\partial B/\partial x = -\mu_0 J_y, \qquad \partial B/\partial y = \mu_0 J_x \tag{1}$$

where J_y and J_x are components of the shielding current density and satisfy the condition of the CSM, $J_y^2 + J_x^2 = |\boldsymbol{J}_c|^2$. To study the effect of anisotropy in $\boldsymbol{J}_c$., we assume the general form

$$|\boldsymbol{J}_c| = J_{co} f(\theta). \tag{2}$$

Here θ refers to the direction of the current density, i.e., $\tan\theta = J_x/J_y = -(\partial B/\partial y)/(\partial B/\partial x)$, and J_{c0} is the critical current density in the absence of anisotropy. In general, J_{c0} could be a known function of the local field B, say, $J_{c0}(B)$. From equations (1) and (2) we have

$$(\partial B/\partial x)^2 + (\partial B/\partial y)^2 = (\mu_0 J_c)^2 = (\mu_0 J_{c0})^2 f(\theta)^2. \tag{3}$$

Solution of equation (3) determines the function $B(x, y)$ that assumes the value B_a on the boundary and gives the distribution of the local field within the sample. It also determines the

contours of constant B or the flux fronts. Before we determine the flux contours, following [12], let us introduce a new variable, say, β, with the dimension of length. In [12] the indefinite integral

$$\beta = \int^{B} \mathrm{d}v/[\mu_0 J_{c0}(v)]$$

was used. We shall work with a definite integral representation of β with zero as the lower limit. If we determine β, we can obtain $B = B(\beta)$ by inverting the defining equation. We shall also denote by β_a the β-value corresponding to B_a, i.e., $B_a = B(\beta_a)$. Further, we will assume that $J_{c0}(B)$ is a monotonically decreasing function of $|B|$. Thus flux contours can be determined from the knowledge of either B or β. The latter satisfies the equation

$$(\partial\beta/\partial x)^2 + (\partial\beta/\partial y)^2 = f(\theta)^2. \tag{3'}$$

A comparison of equation (3′) (that does not involve $J_{c0}(B)$) with equation (3) shows that the shape of the flux fronts is independent of the functional dependence of $J_{c0}(B)$. If J_{c0} is independent of B then β and B are linearly related $B = \mu_0 J_{c0}\beta$. It would be prudent to work with equation (3′) rather than equation (3). Clearly, equation (3′) is a nonlinear first order partial differential equation. Its solution can be obtained [13] as an envelope of its one-parameter family of solutions, which, in turn, is obtained from its *complete integral*, i.e., a solution involving two arbitrary constants. It is easy to see that the function

$$\beta = px + qy + r \tag{4}$$

involving parameters p, q and r, that are independent of x and y, satisfies equation (3) provided

$$p^2 + q^2 = f(\theta)^2 \tag{5}$$

with $\tan\theta = -q/p$. Thus p and q are related. If we also choose the parameter r as a function of p we get a one-parameter family of solutions of equation (3). Alternatively, we choose a parameter ϕ, and write $p = \rho\cos\phi$ and $q = \rho\sin\phi$ and set $r = r(\phi)$. We then have $\theta = -\phi$, and if we choose $\rho = f(\phi)$, equation (5) reduces to an identity. In terms of the parameter ϕ, equation (3) may be written as

$$\beta = \rho(x\cos\phi + y\sin\phi) + r(\phi). \tag{6}$$

For a fixed value of ϕ, equation (6) represents a plane in the (β, x, y) space. The envelope of the one-parameter family of planes represented by equation (6) is obtained as usual by eliminating ϕ between equation (6) and the equation

$$0 = \rho'(x\cos\phi + y\sin\phi) + r'(\phi) + \rho(-x\sin\phi + y\cos\phi) \tag{7}$$

obtained by differentiating equation (6) with respect to the parameter ϕ. In the above equation a prime on a symbol denotes the derivative with respect to ϕ. The solution surface (envelope of surfaces represented by equation (6)) must touch every member of the family. Thus each point on the solution surface corresponds to some value of ϕ. Let us take $x = x(s)$, $y = y(s)$ to be the parametric equations for the boundary of the cross section of the cylindrical sample. The solution will satisfy the boundary condition if $\beta(x(s), y(s)) = \beta_a$, is identically satisfied for all values of the parameter s. Hence $\partial\beta(x(s), y(s))/\partial s$ must vanish for all s. These two requirements determine which member of the family touches the solution surface at the point $(\beta_a, x(s), y(s))$, i.e determines ϕ as a function of s and also the unknown function $r(\phi)$. From equations (6) and (7) we have

$$r(\phi) = \beta_a - \rho(x(s)\cos\phi + y(s)\sin\phi) \tag{6'}$$

$$0 = \rho'(x(s)\cos\phi + y(s)\sin\phi) + r'(\phi) + \rho(-x(s)\sin\phi + y(s)\cos\phi) \tag{7'}$$

valid for all s. Differentiating equation (6′) with respect to s yields

$$\cos\phi(\mathrm{d}x/\mathrm{d}s) + \sin\phi(\mathrm{d}y/\mathrm{d}s) = 0; \tag{6''}$$

equation (6″) provides the relation between ϕ and s, i.e., it determines which member of the family touches the solution surface at the point $(x(s), y(s))$. Equations (6′), (6) and (7) imply

$$\beta - \beta_a = \rho[(x - x(s))\cos\phi + (y - y(s))\sin\phi] \tag{8}$$

and

$$0 = \rho'[(x - x(s))\cos\phi + (y - y(s))\sin\phi] + \rho[-(x - x(s))\sin\phi + (y - y(s))\cos\phi]. \tag{9}$$

Using the relation $\rho = f(\phi)$ and solving equations (8) and (9) for x and y, we get the parametric equations for constant B or the flux contours

$$x = x(s) - (h/\rho)[(\rho'/\rho)\sin\phi + \cos\phi] \tag{10a}$$

$$y = y(s) - (h/\rho)[\sin\phi - (\rho'/\rho)\cos\phi]. \tag{10b}$$

It should be noted that during the virgin curve, $B > 0$ and progressively decreases towards the centre of the sample, and hence for all $J_{c0}(B)$ decreasing with $|B|\beta - \beta_a$ is negative, while during field reversal from the field increasing case $\beta - \beta_a$ is positive over part of the sample. To cover both these cases we have used $h = |\beta - \beta_a|$ in equations (10a) and (10b). The entire sample can be covered by means of flux contours if h is allowed to vary from $h = 0$ at the surface to $h = \beta_p$, at the field for full penetration.

Since we have solved equation (3′) the flux-contour parameter $h = |\beta - \beta_a|$ involves β. In the case of constant J_{c0}, $B = \mu_0 J_{c0}\beta$ and $B_a = \mu_0 J_{c0}\beta_a$. In the general case of field dependent J_{c0}, B is obtained from β by inverting the defining equation for β based on the known field dependence of J_{c0}.

Equations (10), together with equation (6″) that expresses a relation between ϕ and s, represent the general result for flux fronts valid for cylindrical samples of any arbitrary cross section whose boundary is represented by the parametric functions $x = x(s)$, and $y = y(s)$ and for an arbitrary form of anisotropy. In principle, virgin and hysteresis magnetization of the sample can be obtained using these equations. We shall now specialize these equations to elliptic cylinders and elliptic form of anisotropy.

3. Elliptic cylinder and elliptic anisotropy

3.1. The flux contours

The elliptic boundary of the sample (the boundary of the transverse cross section of the cylinder) may be represented by the parametric equations

$$x(s) = a\cos s, \qquad y(s) = b\sin s. \tag{11}$$

The semi-axes of the ellipse are denoted by a and b respectively. Without loss of generality we may assume $a > b$. To describe the anisotropy of $\boldsymbol{J}_c$ we choose in equation (2) the following (elliptic) form of $f(\theta)$:

$$f(\theta) = (\cos^2\theta + \alpha^2\sin^2\theta)^{1/2}. \tag{12}$$

Using equations (11) in (6″) we get the relation between s and ϕ: $\tan s = (b/a)\tan\phi$. We now express equations (10) that govern the shape of the flux fronts in terms of ϕ:

$$x = [(a^2/\Delta) - (h/\rho)\{2 - 1/\rho^2\}]\cos\phi \tag{13a}$$

$$y = [(b^2/\Delta) - (h/\rho)\{2 - (\alpha/\rho)^2\}]\sin\phi \tag{13b}$$

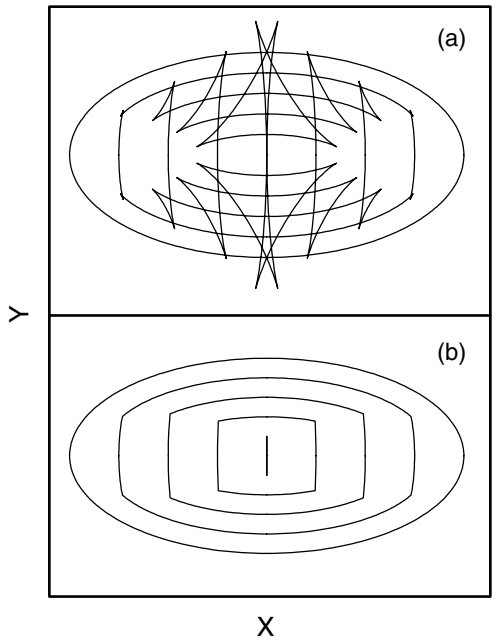

Figure 2. (a) Typical flux contours represented by equations (13) are plotted. The outermost is the sample boundary of the elliptical cross section of the cylinder with semi-axes $a = 1$ and $b = 0.5$. The next one just begins to have double points. All the other contours have visible loops at the double points. These are mathematical solutions. (b) The physically acceptable flux contours obtained from those in (a) by removing the loops at the double points. The anisotropy parameter $\alpha = 2.5$.

where

$$\Delta = (a^2 \cos^2 \phi + b^2 \sin^2 \phi)^{1/2} \tag{14a}$$

$$\rho = f(\phi) = (\cos^2 \phi + \alpha^2 \sin^2 \phi)^{1/2}. \tag{14b}$$

It should be remarked that equation (13) represents mathematical flux fronts which can possibly have double points corresponding to applied field beyond a certain value [2, 12]. The physically acceptable flux fronts must progressively reduce in size and can be obtained from the mathematical flux fronts by dropping out the extraneous portions. Figure 2 should clarify the situation. Figure 2(a) shows the mathematical flux fronts and figure 2(b) shows the physically acceptable ones obtained from figure 2(a).

Equations (13) also determine B_p, the field for full flux penetration. At full penetration, the flux contour reduces to a point (the centre of the sample) or a line that must pass through the centre of the sample. Thus, at full penetration the point $x = y = 0$ lies on the flux contour. A simple algebra using equations (13) and (14) leads to the result that $h_p = |\beta_p - \beta(0)| = \min(a, b\alpha)$, where $\min(u, v)$ stands for the smaller of u and v and β_p is the β-value corresponding to applied field B_p, $B_p = B(\beta_p)$. Hence B_p can be determined.

3.2. Determination of the double points

The form of equations (13) suggests that the flux fronts it represents are symmetric. In other words, the points (x, y), $(-x, y)$, $(-x, -y)$ and $(x, -y)$ all lie on the same flux front. It therefore suffices to consider only the portion of the flux front lying in the first quadrant obtained

by restricting ϕ to the interval $(0, \pi/2)$. To determine a double point let us consider two points (x_1, y_1) and (x_2, y_2) corresponding to the parameter values ϕ_1 and ϕ_2 respectively and seek conditions under which, for $\phi_1 \neq \phi_2$, the equations $x_1 = x_2$ and $y_1 = y_2$ are simultaneously satisfied. These two equations can be simplified making explicit use of equation (13). The equation involving the x coordinate leads to the following conditions:

$$\cos\phi_1 - \cos\phi_2 = 0 \tag{15a}$$

$$\frac{a^2}{\Delta_1} - \frac{h}{\rho_1}\left(2 - \frac{1}{\rho_1^2}\right) = \cos\phi_2(\cos\phi_2 + \cos\phi_1)\left[\frac{a^2(a^2 - b^2)}{\Delta_1\Delta_2(\Delta_1 + \Delta_2)} + \frac{h(\alpha^2 - 1)(2 - g)}{\rho_1\rho_2(\rho_1 + \rho_2)}\right]. \tag{15b}$$

We have used the notation $\Delta_1 = \Delta(\phi_1)$, $\rho_1 = \rho(\phi_1)$ etc, and $g = (\rho_{1.}^2 + \rho_2^2 + \rho_1\rho_2)/\rho_1^2\rho_2^2$. The equation involving the y-coordinate leads to

$$\sin\phi_1 - \sin\phi_2 = 0 \tag{16a}$$

$$\frac{b^2}{\Delta_1} - \frac{h}{\rho_1}\left(2 - \frac{\alpha^2}{\rho_1^2}\right) = \sin\phi_2(\sin\phi_2 + \sin\phi_1)\left[\frac{b^2(b^2 - a^2)}{\Delta_1\Delta_2(\Delta_1 + \Delta_2)} - \frac{h(\alpha^2 - 1)(2 - \alpha^2 g)}{\rho_1\rho_2(\rho_1 + \rho_2)}\right]. \tag{16b}$$

The points (x_1, y_1) and (x_2, y_2) would represent a double point if ϕ_1 and ϕ_2 simultaneously satisfied one of equations (15) and one of equations (16). Since we are looking for a solution $\phi_1 \neq \phi_2$, equation (15a) can be satisfied if we choose $\phi_2 = -\phi_1$. Then equation (16a) cannot be satisfied. Thus a double point corresponding to $\phi_2 = -\phi_1$ must be a solution of equations (15a) and (16b). But for $\phi_2 = -\phi_1$, the right-hand side of (16b) vanishes, hence the double point corresponds to the solution of

$$\frac{b^2}{\Delta_1} - \frac{h}{\rho_1}\left(2 - \frac{\alpha^2}{\rho_1^2}\right) = 0. \tag{16b′}$$

However, under the condition (16b') it follows from equation (13b) that $y_1 = y_2 = 0$. Thus the double point lies on the major axis of the elliptical cross section. The entire flux contour has only two double points. Since there is only one variable, we may drop the suffix 1 without any confusion and solve equation (16b') for h and write

$$h = b^2\rho/[\Delta(2 - (\alpha/\rho)^2]. \tag{17}$$

Equation (17) defines h as a function of ϕ, involving the parameters a, b and α. A simple calculation of eliminating ϕ between Δ and ρ leads to the relation

$$\frac{\Delta^2}{\rho^2} = \left(\frac{b^2 - a^2\alpha^2}{1 - \alpha^2}\right)\frac{1}{\rho^2} + \frac{a^2 - b^2}{(1 - \alpha^2)}. \tag{18}$$

We have assumed that $a > b$. The above relation implies that for $\alpha < 1$ but $a\alpha > b$, h is a monotonically decreasing function of ρ, implying that it is a monotonically increasing function of ϕ. The smallest value $h = h_{\min}$ is obtained for $\phi = 0$ in (17). Thus, for $h > h_{\min}$ there is a nonzero value of ϕ that can be obtained by solving equation (17) numerically. That determines ϕ_1 and $\phi_2 = -\phi_1$. For this case, physically acceptable flux contours can be obtained and are shown in figure 3(a). They develop into a spindle shape and may be compared with the flux contours for the isotropic case, namely $\alpha = 1$ (figure 3(b)).

The above analysis fails if $\alpha > 1$ and also for values of α so small that $a\alpha < b$. In these cases $h_{\min}$ occurs in equation (17) at a finite value of ϕ and this contradicts the assumption that the double point is on the major axis. In these cases the double point must correspond to a solution of equations (15b) and (16b). It is clear that at the onset of formation of the loop

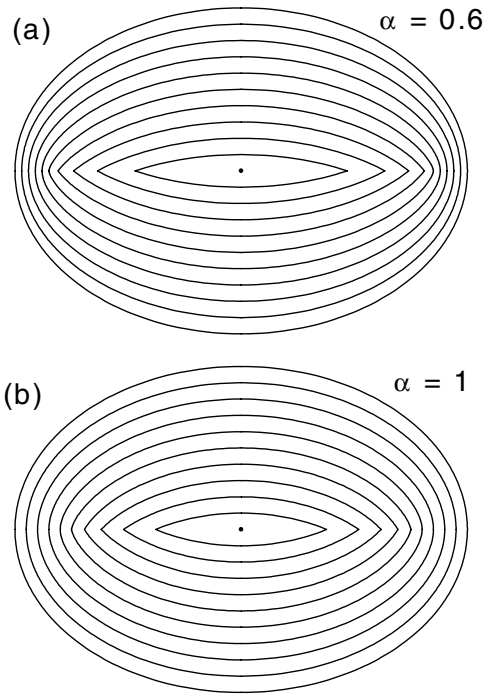

Figure 3. (a) Flux contours for the elliptical cylinder, with semi-axes $a = 1$ and $b = 0.5$ with (a) $\alpha = 0.8$ and (b) for the isotropic sample, i.e., $\alpha = 1$.

(or the occurrence of a double point) $h = h_{\min}$ which should correspond to $\phi_2 = \phi_1$. Hence to get an expression for $h_{\min}$ we must solve equations (15*b*) and (16*b*) under the substitution $\phi_2 = \phi_1 = \phi$ and seek the minimum of the expression. This gives us

$$h = a^2b^2\rho^3/[\Delta^3(2(1+\alpha^2) - 3(\alpha/\rho)^2]. \tag{19}$$

The function on the right-hand side of the above equation is not monotonic as a function of ρ or ϕ. It attains a minimum ($h_{\min}$) at a value of $\rho = \rho_{\min}$, given by

$$\rho_{\min}^2 = \frac{5\alpha^2(b^2 - a^2\alpha^2)}{2\{b^2(2\alpha^2+1) - a^2\alpha^2(2+\alpha^2)\}}. \tag{20}$$

The corresponding value of ϕ can be determined by solving (14*b*). For $h > h_{\min}$ we must solve equations (15*b*) and (16*b*) as simultaneous transcendental equations to determine ϕ_1 and ϕ_2. These can be solved only numerically. To this end we first obtained a relation involving only ϕ_1 and ϕ_2 by eliminating h from equations (15*b*) and (16*b*) and cancelling a factor that vanishes when $\phi_1 = \phi_2$, and also obtained a relation, symmetric in ϕ_1 and ϕ_2 from equations (15*b*) and (16*b*) for determining h. The flux contours obtained following this procedure are shown in figure 2(b).

3.3. Magnetization curves

The magnetization of the sample is calculated using the definition

$$\mu_0 m = (1/A)\int (B - B_a)\,\mathrm{d}x\,\mathrm{d}y = -B_a + (1/A)\int B\,\mathrm{d}x\,\mathrm{d}y. \tag{21}$$

Integration is performed over the cross sectional area A of the sample. Let us first consider magnetization during the virgin curve for a zero-field-cooled sample. For this case we have $\beta - \beta_a = -h$. On the sample surface $B = B_a$, hence, $h = 0$. Similarly, on and within the innermost flux contour $B = 0$, implying $h = \beta_a$. It is advantageous to change the variables of integration from (x, y) to (h, ϕ) as per equation (13). For a given applied field B_a, variation of h may be restricted only to the range $(0, \beta_a)$ beyond which $B = 0$. The surface elements are related through J, the Jacobian of the transformation, and can be calculated in a straightforward manner; the result is

$$J(h, \phi) = h[(3\alpha^2/\rho^6) - \{2(1 + \alpha^2)/\rho^4\}] + a^2b^2/\Delta^3\rho. \tag{22}$$

The virgin magnetization can be written as

$$\mu_0 m_v = -B_a + \frac{1}{A}\int B\,J\,\mathrm{d}h\,\mathrm{d}\phi = -B_a - \frac{1}{\pi ab}\int_0^{\beta_a} \mathrm{d}h\; B(\beta_a - h)\int J\,\mathrm{d}\phi. \tag{23}$$

We noted earlier that flux contours develop corners for h greater than a certain $h_{\min}$. These correspond to the double points on the mathematical flux contours. For $h > h_{\min}$ the physical flux fronts are obtained by omitting a certain range of ϕ values, say (ϕ_1, ϕ_2). We need to determine the values of ϕ_1 and ϕ_2 for obtaining the physical flux fronts. The symmetry of the integrand suffices the evaluation of the ϕ integral over quarter range, namely 0 to $\pi/2$, of which the interval (ϕ_1, ϕ_2) is to be omitted. It is clear from the expression (22) for J that we need to evaluate the indefinite integrals of ρ^{-4}, ρ^{-6} and $\Delta^{-3}\rho^{-1}$ over the variable ϕ. The former two can be obtained in terms of elementary functions and the latter can be expressed in terms of incomplete elliptic functions. We recall the definitions of ρ and Δ given in equation (14) and give the final results.

$$\int \frac{\mathrm{d}\phi}{\rho^4} = \frac{1}{2\alpha^3}\left[(1 + \alpha^2)\tan^{-1}(\alpha\tan\phi) + \frac{(\alpha^2 - 1)\alpha\sin\phi\cos\phi}{\cos^2\phi + \alpha^2\sin^2\phi}\right] \tag{24}$$

$$\int \frac{\mathrm{d}\phi}{\rho^6} = \frac{1}{8\alpha^5}\left[(3 + 2\alpha^2 + 3\alpha^4)\tan^{-1}(\alpha\tan\phi) + \frac{4(\alpha^4 - 1)\alpha\sin\phi\cos\phi}{\cos^2\phi + \alpha^2\sin^2\phi} + \frac{(\alpha^2 - 1)^2\alpha\sin\phi\cos\phi[\cos^2\phi - \alpha^2\sin^2\phi]}{[\cos^2\phi + \alpha^2\sin^2\phi]^3}\right] \tag{25}$$

$$\int \frac{\mathrm{d}\phi}{\Delta^3\rho} = \frac{a(\alpha^2 - 1)}{a^2\alpha^2 - b^2}F\left(\theta, \frac{\sqrt{b^2 - a\alpha^2}}{b}\right) + \frac{a^2 - b^2}{a(a^2\alpha^2 - b^2)}E\left(\theta, \frac{\sqrt{b^2 - a\alpha^2}}{b}\right) \tag{26}$$

for $b > a\alpha$ and $\tan\theta = (b/a)\tan\phi$; $E(\theta, k)$ and $F(\theta, k)$ are the incomplete elliptic functions of first and second kinds of modulus k. For the other case, namely $a\alpha > b$, we have

$$\int \frac{\mathrm{d}\phi}{\Delta^3\rho} = \frac{(\alpha^2 - 1)}{a\alpha(a^2\alpha^2 - b^2)}F\left(\theta, \frac{\sqrt{a^2\alpha^2 - b^2}}{a\alpha}\right) + \frac{a^2 - b^2}{ab^2(a^2\alpha^2 - b^2)}E\left(\theta, \frac{\sqrt{a^2\alpha^2 - b^2}}{a\alpha}\right) - \frac{(a^2 - b^2)\sin\theta\cos\theta}{a^2b^2\sqrt{a^2\alpha^2\cos^2\theta + b^2\sin^2\theta}} \tag{27}$$

where $\tan\theta = \alpha\tan\phi$. For $b = a\alpha$ the integral is elementary and has the value

$$\int \frac{\mathrm{d}\phi}{\Delta^3\rho} = \frac{1}{b^3}\left[\frac{(\alpha^2 + 1)}{2}\theta + \frac{(\alpha^2 - 1)}{2}\sin\theta\cos\theta\right]. \tag{28}$$

Using the values of integrals (24–(28) in the expression (23) for virgin magnetization and the expression (22) for J we have calculated the virgin magnetization. It reaches its saturation value m_s at the field B_p for full penetration. For $B_a > B_p$ $m_v = m_s$.

Magnetization under reversal of field from some field B_m can be expressed in terms of virgin magnetization. Let us denote $m_v(B_a)$ the functional form for the virgin magnetization. On the virgin curve, for $B_a = B_m$, $m = m_v(B_m)$. Let the applied field now be reduced to, say, $B_a = B_m - \Delta B$. The shielding currents near the surface region will reverse their sense of flow, so as to shield the interior from the change of field $-\Delta B$. Hence we can write magnetization under field reversal $m_\downarrow(B_m - \Delta B) = m_v(B_m) - 2m_v(\Delta B)$. We can increase $-\Delta B$ up to B_m corresponding to applied field decreased to $-B_m$. To complete the loop the field is increased from $-B_m$ to B_m. The magnetization during the field increasing part of the loop is obtained using $m_\uparrow(B_a) = -m_\downarrow(-B_a)$.

3.3.1. Field dependent critical current density. The calculation of magnetization presented above is directly applicable to the case of constant critical current density. As remarked earlier, field dependence of J_c does not alter the shape of flux contours. It should be remembered that, in the general case of field dependent J_c, the flux contours are labelled by the parameter $h = |\beta_a - \beta|$, with β as defined earlier. The above formula for magnetization (equation (23)) can then be utilized. For the exponential model we have $J_{c0} = J_{c0}(0)\exp(-|B|/B_0|)$, where B_0 is a parametric field that governs the decay of the current density. We calculate β from the definition

$$\beta = \int_0^B \frac{\mathrm{d}v}{\mu_0 J_{c0}(v)} = \pm\frac{B_0}{\mu_0 J_{c0}}(\exp(|B|/B_0) - 1). \tag{29}$$

Thus for the virgin curve we have both $B > 0$ and $B_a > 0$, and we have

$$\beta_a = (B_0/\mu_0 J_{c0})[\exp(B_a/B_0) - 1], \qquad \beta = (B_0/\mu_0 J_{c0})[\exp(B/B_0) - 1]$$

and consequently

$$h = (B_0/\mu_0 J_{c0})[\exp(B_a/B_0) - \exp(B/B_0)] \tag{30a}$$

or equivalently

$$B = B_0 \ln[\exp(B_a/B_0) - (\mu_0 J_{c0} h/B_0)]. \tag{30b}$$

The flux-contour parameter h increases from zero to its maximum value β_a, corresponding to $B = 0$. Equation (30*b*) determines B in terms of h for $h < \beta_a$. For $h > \beta_a$, $B = 0$. Virgin magnetization can be determined form equation (21). The virgin curve extends even beyond the field B_p corresponding to full penetration. Since $B > 0$ everywhere, the B-profile is given by equation (30*b*). This part of the virgin curve merges with the field increasing envelope curve obtained below.

During the envelope curve shielding currents flow throughout the sample in one sense. On the field increasing envelope, the local field B decreases towards the centre of the sample. If we write $\beta_p = (B_0/\mu_0 J_{c0})[\exp(B_p/B_0) - 1]$ corresponding to the field for full penetration, we have three situations, namely, (i) $B_a < 0$, (ii) $0 < B_a < B_p$ and (iii) $B_a > B_p$.

If $B_a < 0$, then $B < 0$ everywhere within the sample and using the appropriate expression for β_a and β we have

$$h = (B_0/\mu_0 J_{c0})[\exp(-B/B_0) - \exp(-B_a/B_0)]. \tag{31a}$$

The profile B can be determined for this case by inverting the above equation.

$$B = -B_0 \ln[1 + (\mu_0 J_{c0}/B_0)\{h - \beta_a\}]. \tag{31b}$$

For the case (ii) ($B_a > 0$) we refer to the above development of the field profile for the virgin curve. There we should allow the profile for B to continue beyond $h = \beta_a$ by letting B to be

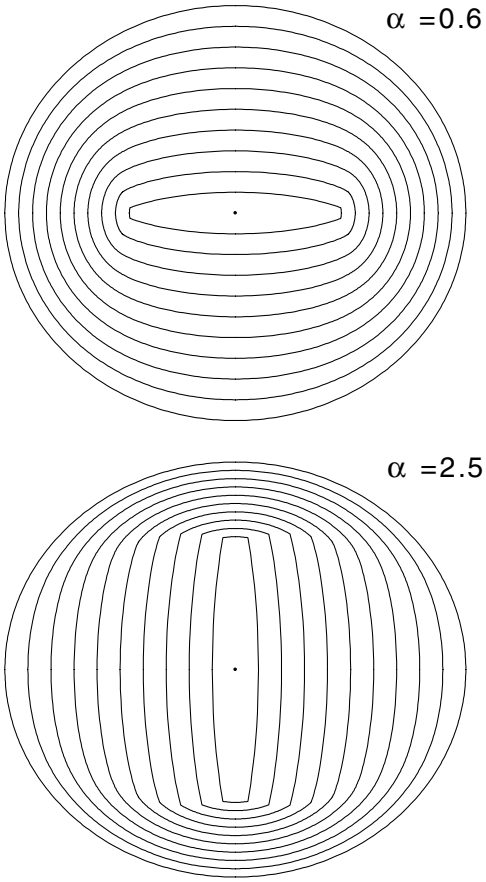

Figure 4. A comparison of flux contours for a circular cylinder with $\alpha = 2.5$ and 0.6.

negative (instead of setting $B = 0$) and use the expression for β relevant to the case $B < 0$, namely, $\beta = -(B_0/\mu_0 J_{c0})[\exp(-B/B_0) - 1]$; we have

$$h = [\beta_a + (B_0/\mu_0 J_{c0})\{\exp(-B/B_0) - 1\}] \tag{32a}$$

or

$$B = -B_0 \ln[1 + (\mu_0 J_{c0}/B_0)\{h - \beta_a\}]. \tag{32b}$$

Thus for $B_a < B_p$, we use equation (30*b*) to determine B for $h < \beta_a$ and equation (32*b*) for $h > \beta_a$. For $B_a > B_p$, $B > 0$ throughout the sample and can be obtained from equation (30*b*). Once the local field profile is determined the envelope magnetization can be obtained.

To get a hysteresis loop, we must calculate magnetization by varying the applied field from some value, say B_m, to $-B_m$ and then increasing the field back to B_m. Thus it is imperative to determine the magnetization on reversal of field. Reversal of field from a point on the virgin curve corresponding to ($B_m < B_p$) leads to a small loop.

Let us start with the initial profile at the applied field B_m given by equation (30*b*) with $B_a = B_m$ and B decreasing to zero at the value of $h = \beta_m = (B_0/\mu_0 J_{c0})[\exp(B_m/B_0) - 1]$. Let the applied field be decreased to $B_a < B_m$. The sense of induced currents near the surface reverses. The local field B increases from its value B_a at the surface. The increasing profile

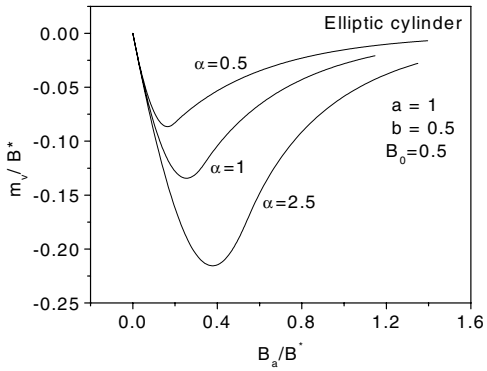

Figure 5. Virgin curves for the exponential model $J_{c0} \sim \exp(-|B|/B_0|$ with $B_0 = 0.5B^*$, where $B^* = \mu_0 J_{c0} a$, for different values of the anisotropy parameter α are shown. The elliptic cylindrical sample has semi-axes $a = 1.0$ and $b = 0.5$.

meets the initial profile at some local field, say, B', with the value of the flux front parameter h'. The field profile B remains unchanged for $h > h'$. Thus B_a and h' must be related. It is clear that as we vary h' from zero to β_m the applied field will vary from B_m to $-B_m$. If $B_a > 0$, $B > 0$, the field increasing part of the profile can be expressed in terms of h and h'. From the initial profile we have

$$h' = (B_0/\mu_0 J_{c0})[\exp(B_m/B_0) - \exp(B'/B_0)] \tag{33a}$$

and for the field increasing profile near the surface we have

$$h = (B_0/\mu_0 J_{c0})[\exp(B/B_0) - \exp(B_a/B_0)]. \tag{33b}$$

For $B = B'$ we have

$$h' = (B_0/\mu_0 J_{c0})[\exp(B'/B_0) - \exp(B_a/B_0)]. \tag{33b'}$$

Eliminating B' between (33a) and (33b') we get

$$\exp(B_a/B_0) = \exp(B_m/B_0) - 2(\mu_0 J_{c0}/B_0)h'). \tag{34}$$

The increasing profile with $B' > B > B_a$ is determined by inverting (33b) and using (34)

$$B = B_0 \ln[\exp(B_m/B_0) - (\mu_0 J_{c0}/B_0)\{2h' - h\}]. \tag{35}$$

If $B_a < 0$ then $B < 0$ near the surface (close to $h = 0$), and vanishes for $h = h'_0$ obtained from equation (35) by setting $B = 0$.

$$h'_0 = (B_0/\mu_0 J_{c0})[1 - \exp(B_m/B_0)] + 2h'. \tag{36}$$

For $h < h'_0$ the local field $B < 0$ and also $B_a < 0$. Following the procedure as outlined above we get

$$B = -B_0 \ln[\exp(1 + (\mu_0 J_{c0}/B_0)\{h'_0 - h\}]. \tag{37}$$

For $h' > h > h'_0$, $B > 0$ and is given by equation (35).

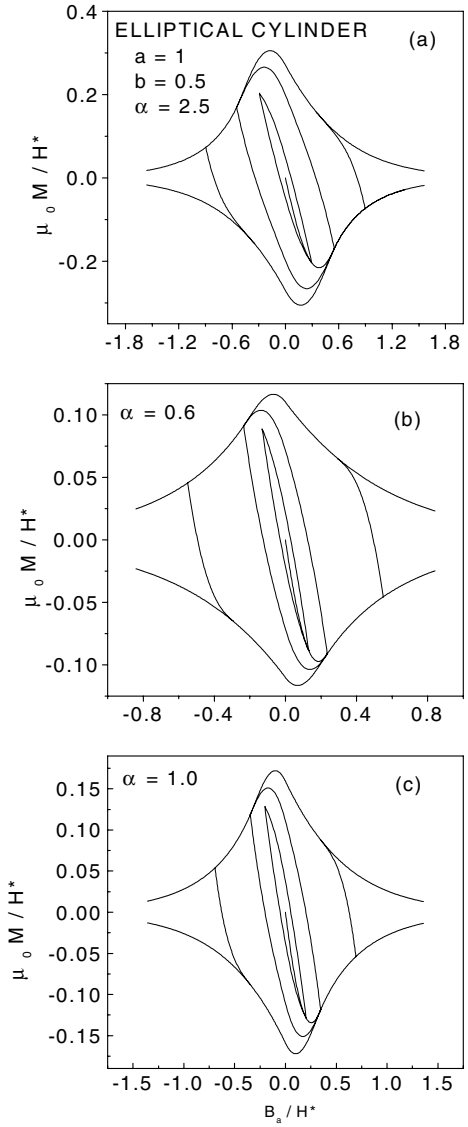

Figure 6. The virgin curve and the envelope curves are shown for an elliptical cylinder with semi-axes $a = 1.0$ and $b = 0.5$ and the exponential model for J_c. (a) For $\alpha = 2.5$, the field for full penetration $B_p = 0.549B^*$. The small and large hysteresis loops are also shown corresponding to the reversal fields $B_m = 0.2939B^*$, $B_m = B_p$ and $B_m = 0.8959B^*$ respectively. (b) The same as (a) for $\alpha = 0.6$. For this case $B_p = 0.235B^*$ and the reversal fields are $B_m = 0.1312B^*$, $B_m = B_p$ and $B_m = 0.5148B^*$. (c) We also show hysteresis curves for a symmetric sample ($\alpha = 1$) for comparison. For this case $B_p = 0.3466B^*$ and the reversal fields are $B_m = 0.2027B^*$, $B_m = B_p$ and $B_m = 0.6931B^*$.

4. Results and discussion

We have presented a general method to obtain flux contours and magnetization curves for cylindrical samples of arbitrary cross section, in parallel geometry, with anisotropic critical current density. The method is applied to cylindrical samples of elliptical cross-section and an elliptic form of the anisotropy.

Mathematical solutions to flux contours develop double points. We have presented a prescription to locate the double point and get physically acceptable flux contours. Figure 2 illustrates the procedure for an elliptical cylinder with semi-axes $a = 1$ and $b = 0.5$ and the anisotropy parameter $\alpha = 2.5$. For $\alpha < 1$ but $a\alpha > b$ the character of the flux contours is similar to those in an isotropic sample with $b < a$. Figure 3 illustrates this fact.

The effect of anisotropy would be best brought out if the sample were symmetrical. For a circular cylinder of radius $a = 1$, flux contours are plotted in figure 4 for two values of the anisotropy parameter $\alpha = 2.5$ and 0.6. For the isotropic case ($\alpha = 1$) it is well known that the flux contours are concentric circles. There is a qualitative change in the shape of the flux contours for $\alpha \neq 1$. It is seen that figure 4(b) is qualitatively similar to figure 2(b), while figure 4(a) is similar to (b) rotated by 90°. The manner in which the flux contours evolve, as the field penetrates the sample, is different for the two cases $\alpha > 1$ and $\alpha < 1$ as seen from figure 4. This is to be expected from the θ-dependence of $|\boldsymbol{J}_c|$ (cf equations (2) and (12)).

Virgin magnetization curves are presented in figure 5 for anisotropic critical current density that decays exponentially with the local field, for three values of the anisotropy parameter α. A comparison of magnetization hysteresis loops is presented in figure 6. Here we plot the virgin curve, the envelope curves and the reversal curves for various reversal fields. The size of the hysteresis loop increases with α.

For thin samples, to first order in d/L (d is the thickness and L is the lateral dimension transverse to the applied field), the effect of anisotropy in the critical current density can be taken into account by an effective field dependence of the critical current density [14]. For cylindrical samples and elliptical form of the anisotropy treated here such a replacement is not possible. Thus the fortunate circumstance mentioned above do not hold for thick samples.

Finally, the case of elliptic cylindrical samples and the elliptic anisotropy was chosen for the purpose of illustration and the method presented is applicable to cylinders in general and for other forms of anisotropy in $\boldsymbol{J}_c$. The method was also applied to cylinders of rectangular cross-section. For rectangular cylinders we found that (in a parallel geometry) shape dominates anisotropy in that the flux contours are similar to those for an isotropic rectangular cylinder.

References

[1] Bean C P 1962 *Phys. Rev. Lett.* **8** 250
Bean C P 1964 *Rev. Mod. Phys.* **36** 31
[2] Campbell A M and Evetts J E 1972 *Adv. Phys.* **21** 199
[3] Bhagwat K V and Chaddah P 1989 *Pramana J. Phys.* **33** 521
Bhagwat K V and Chaddah P 1992 *Physica* C **190** 444
Bhagwat K V and Chaddah P 1994 *Physica* C **224** 155
Bhagwat K V and Chaddah P 1997 *Physica* C **280** 52
[4] Navarro R and Campbell L J 1991 *Phys. Rev.* B **44** 10146
[5] Telchow K L and Koo L S 1994 *Phys. Rev.* B **50** 6923
[6] McDonald J and Clem J R 1996 *Phys. Rev.* B **53** 8643
[7] Brandt E H 1996 *Phys. Rev.* B **54** 4246
[8] Küpfer H, Ravikumar G, Wolf Th, Zhukov A A, Will A, Leibrock H, Meier-Hirmer R, Wühl H and de Groot P A J 2002 *Phys. Rev.* B **66** 064512
[9] Sen S, Singh A, Aswal D K, Gupta S K, Yakhmi J V, Sahni V C, Choi E-M, Kim H-J, Kim K H P, Lee H-S, Kang W N and Lee S-I 2002 *Phys. Rev.* B **65** 214521
[10] Schuster Th, Kuhn H, Brandt E H and Klaumünzer S 1997 *Phys. Rev.* B **56** 3413
[11] Badia A and López C 2002 *Preprint* cond-mat/0209494
[12] Bhagwat K V and Chaddah P 1991 *Phys. Rev.* B **44** 6950
[13] Sneddon I N 1957 *Elements of Partial Differential Equations* (New York: McGraw-Hill) pp 59–60
[14] Mikitik G P and Brandt E H 2000 *Phys. Rev.* B **62** 6812